GDCh Research Article Angewandte International Edition Chemie www.angewandte.org

Check for updates

How to cite: *Angew. Chem. Int. Ed.* **2024**, *63*, e202407281
doi.org/10.1002/anie.202407281

Copper Catalysis Hot Paper

Copper-Catalyzed Dearomative 1,2-Hydroamination

Christopher W. Davis, Yu Zhang, Yanrong Li, Matteo Martinelli, Jingyang Zhang, Chad Ungarean, Petra Galer, Peng Liu, and David Sarlah**

Abstract: Catalytic olefin hydroamination reactions are some of the most atom-economical transformations that bridge readily available starting materials–olefins and high-value-added amines. Despite significant advances in this field over the last two decades, the formal hydroamination of nonactivated aromatic compounds remains an unsolved challenge. Herein, we report the extension of olefin hydroamination to aromatic π-systems by using arenophile-mediated dearomatization and Cu-catalysis to perform 1,2-hydroamination on nonactivated arenes. This strategy was applied to a variety of substituted arenes and heteroarenes to provide general access to structurally complex amines. We conducted DFT calculations to inform mechanistic understanding and rationalize unexpected selectivity trends. Furthermore, we developed a practical, scalable desymmetrization to deliver enantioenriched dearomatized products and enable downstream synthetic applications. We ultimately used this dearomative strategy to efficiently synthesize a collection of densely functionalized small molecules.

Introduction

Amines are a ubiquitous functional group in organic chemistry due to their prevalence in biologically active molecules and pharmaceutical agents, with over 84% of FDA-approved small molecule drugs containing at least one nitrogen atom.[1] While the synthesis of amines is traditionally achieved using nucleophilic substitution or reductive amination, these reactions can result in poor selectivity and produce superstoichiometric waste byproducts, prompting extensive investigation into alternative catalytic processes.[2] Among various modern methods of amine synthesis, the hydroamination of an olefin represents an efficient and atom-economical strategy for the construction of complex amines.[3] This transformation couples two abundant feedstock chemicals without the need for prefunctionalization and provides valuable aliphatic amines relevant to medicinal chemistry.

Olefin hydroamination has seen major advances during the last two decades, which greatly expanded the range of accessible olefin and amine partners.[4] On the other hand, hydroamination of aromatic systems has remained largely out of reach due to the high resonance stabilization associated with aromaticity and the kinetic intractability of migratory insertion and nucleometallation steps.[5] Although addition of nitrogen functionality is well-documented using dearomative strategies involving reactive phenols and indoles,[6] direct dearomative hydroamination of benzene has only been reported once. In this example, UV irradiation of benzene in the presence of aliphatic amines (Scheme 1a) delivered hydroamination products by addition of the N–H functionality across the arene.[7] However, this method has not seen many synthetic applications since it gave low conversions and generated inseparable constitutional isomers and byproducts. More recently, arene–metal complexes have been employed to perform dearomative amination of nonactivated arenes (Scheme 1b).[8] While these methods rapidly increase molecular complexity, they require stoichiometric use of metals.

In recent years, we and others have advanced the use of arenophiles to achieve dearomative functionalization of nonactivated arenes.[9] Under visible-light irradiation, simple arenes like benzene (**1a**) undergo a [4+2] cycloaddition with photoexcited 4-methyl-1,2,4-triazoline-3,5-dione (MTAD, **2**) and the intermediate cycloadducts can be intercepted through in situ olefin functionalization[10] or transition-metal catalyzed ring opening.[11] Moreover, we recently took inspiration from Cu-catalyzed hydroamination of olefins and established a proof-of-concept involving arenophile-medi-

[*] C. W. Davis,[+] Y. Li, J. Zhang, C. Ungarean, P. Galer, Prof. Dr. D. Sarlah
Department of Chemistry
University of Illinois
Urbana, IL 61801, USA
E-mail: sarlah@illinois.edu

Y. Zhang,[+] Prof. Dr. P. Liu
Department of Chemistry
University of Pittsburgh
Pittsburgh, PA 15260, USA
E-mail: pengliu@pitt.edu

M. Martinelli, Prof. Dr. D. Sarlah
Department of Chemistry
University of Pavia
Pavia, LOM 27100, IT

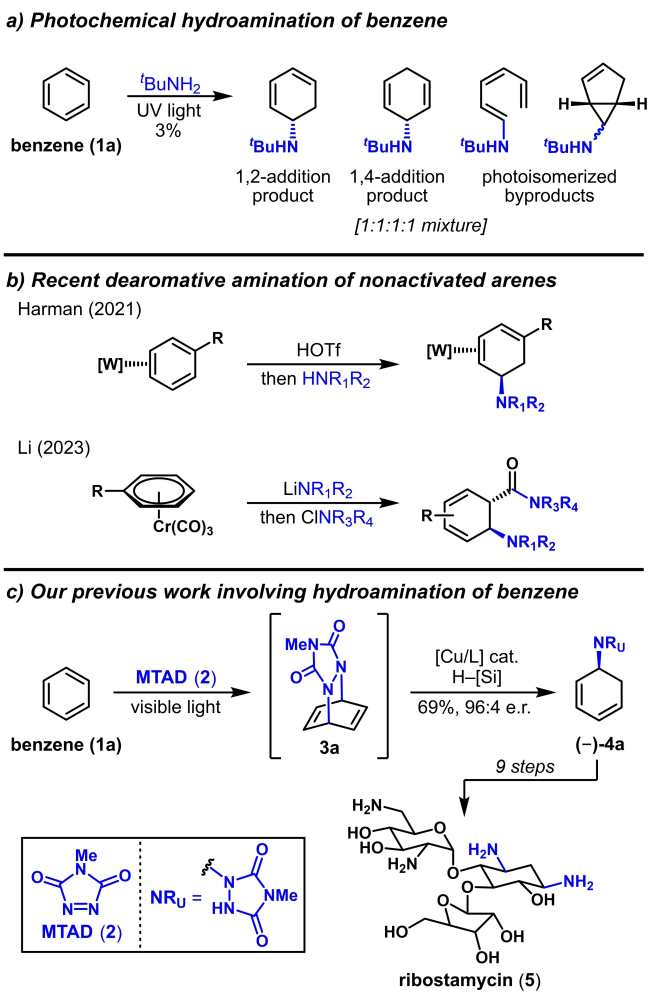

Scheme 1. (a) Previously reported hydroamination of benzene. (b) Recent dearomative amination reactions of nonactivated arenes. (c) Cu-catalyzed dearomative 1,2-hydroamination of benzene in the context of synthesis of ribostamycin (**5**).

ated dearomative 1,2-hydroamination of benzene (Scheme 1c).[12] This approach could be formally seen as an arenophile-assisted isolation of an olefin component from an aromatic system through *para*-cycloadduct **3a**, followed by a catalytic hydrocupration event. The resultant aminodiene **4a** served as a key intermediate that enabled the enantioselective total synthesis of the aminoglycoside antibiotic ribostamycin (**5**).

Considering the lack of direct dearomative hydroaminations and the structural complexity they create, we decided to fully explore this process beyond benzene. In addition to establishing the scope and generality, one of our main objectives included realization of a more practical and reliable protocol. Herein we report the result of these efforts: a general and efficient dearomative 1,2-hydroamination of nonactivated arenes. During these studies, we observed divergent regioselectivity in reactions with substituted arenes, seemingly based on the electronic character of the substituents, which was investigated computationally. We also screened for alternative chiral ligands that provided high levels of enantioinduction with several arenes, thereby enabling gram-scale synthetic applications. Furthermore, we demonstrated the synthetic utility of this dearomative hydroamination by elaboration of the products into a diverse collection of polyfunctionalized small molecules.

Results and Discussion

Optimization of Reaction Conditions

We commenced our optimization studies by formation of cycloadduct **3a** from benzene (**1a**), which was subjected to several conditions established for hydrocupration of olefins (Table 1, see Supporting Information, Table S1, for full optimization details).[13] During our initial screening, we identified several important features of this dearomative process that guided further optimization efforts: 1) copper(I) thiophene-2-carboxylate (CuTC) was identified as the optimal copper precursor (Entries 1 and 2); 2) *N*-heterocyclic carbene (NHC) based ligands generally outperformed bisphosphines (Entries 2 and 3), both ligand classes commonly used in CuH-mediated reactions;[14] 3) temperature

Table 1: Selected optimization studies.[a]

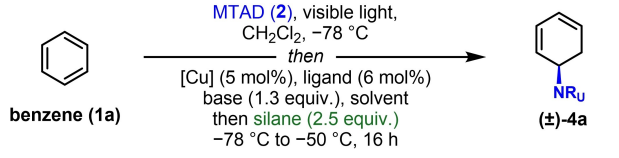

entry	[Cu] (5 mol %)	ligand (6 mol %)	base (1.3 equiv.)	silane (2.5 equiv.)	solvent	yield (%)[b]
1	Cu(OAc)	BINAP	KO^{t}Bu	DEMS	PhMe	12
2	CuTC	BINAP	KO^{t}Bu	DEMS	PhMe	13
3	CuTC	IAd·HBF$_4$	KO^{t}Bu	DEMS	PhMe	29
4	CuTC	ICy·HBF$_4$	KO^{t}Bu	DEMS	PhMe	61
5	CuTC	IPr·HCl	KO^{t}Bu	DEMS	PhMe	68
6	**CuTC**	**IMes·HCl**	**KO^{t}Bu**	**DEMS**	**PhMe**	**75**
7	CuTC	IMes·HCl	NaO^{t}Bu	DEMS	PhMe	44
8	CuTC	IMes·HCl	KO^{t}Bu	PhSiH$_3$	PhMe	< 5
9	CuTC	IMes·HCl	KO^{t}Bu	TMDS	PhMe	< 5
10	CuTC	IMes·HCl	KO^{t}Bu	HMTS	PhMe	< 5
11	CuTC	IMes·HCl	KO^{t}Bu	DEMS	Et$_2$O	72

ligands: IAd·HBF$_4$ (R = 1-adamantyl), ICy·HBF$_4$ (R = cyclohexyl); IPr·HCl (Ar = 2,6-(^{i}Pr)$_2$C$_6$H$_3$), IMes·HCl (Ar = mesityl)

silanes: DEMS, TMDS, HMTS

[a] Standard reaction conditions: MTAD (**2**, 0.5 mmol, 1.0 equiv.), benzene (**1a**, 5.0 mmol, 10 equiv.), CH_2Cl_2 (0.1 M), visible light, −78 °C, 12 h; then solution of catalyst ([Cu] (5 mol %), ligand (6 mol %), base (1.3 equiv.), solvent (2.0 mL)); then silane (2.5 equiv.) added slowly dropwise (see Supporting Information for details). [b] Reported yields were determined by ^{1}H NMR of reaction mixtures after acid–base extraction using nitromethane as internal standard. TMS = trimethylsilyl.

had a pronounced effect on reaction performance, with −50 °C found to be the most effective for high conversions. Taking these points into consideration, we evaluated different NHC ligands (Entries 3–6) and quickly identified 1,3-bis(mesityl)imidazolinium chloride (IMes·HCl) as an optimal choice, furnishing **4a** in 75 % yield (Entry 6).

Further experiments revealed that other bases failed to provide high yields of the desired product, with even the choice of cation proving critical for optimal reactivity (Entry 7, NaO^{t}Bu instead of KO^{t}Bu).[15] Alternate silanes, such as phenylsilane, tetramethyldisiloxane (TMDS), and heptamethyltrisiloxane (HMTS) each failed to provide **4a** (Entries 8–10).[16] Minimal sensitivity to solvent was displayed, with diethyl ether providing only a slightly diminished yield (Entry 11). Importantly, these studies also revealed that slow dropwise addition of silane was crucial to mitigating the exothermicity of copper hydride formation, which was found to significantly impact yield and reproducibility.[17]

Dearomative 1,2-Hydroamination of Arenes and Investigation of Selectivity

With optimized conditions in hand, we examined the scope of benzene derivatives (Scheme 2). In addition to **4a**, alkyl-substituted arenes provided products **4b**–**4d** in moderate to good yields. Chloride (**4c**) and methyl ester (**4d**) substituents were tolerated under the reaction conditions. Curiously, while **4b** and **4c** were obtained as single isomers with a relative 1,6-relationship between the alkyl substituent and urazole moiety (numbering based on 1,2-hydroamination of olefin), **4d** formed as a separable mixture of 1,6- and 1,3-constitutional isomers (see Supporting Information for details). Furthermore, products **4e** and **4f** derived from trimethylphenylsilane (**1e**) and trifluorotoluene (**1f**), respectively, were both exclusively 1,3-substituted. Interestingly, fluorobenzene (**1g**) provided the unique product **4g** with 1,4-substitution, implying that the initial arene–arenophile cycloaddition for this substrate establishes a bridgehead fluoride (cycloadduct **3g**).[18] Although arenes substituted with electron-withdrawing carbonyl-based substituents do not engage in cycloaddition, dearomatized products **4h** and **4i** were obtained from arenes **1h** and **1i** with protected carbonyl functionalities, and displayed a 1,3-substitution pattern. These optimized conditions also proved effective on gram scale, with **4a** obtained in 72 % yield. The dienes **4** were found to be unstable during chromatography due to facile rearomatization, but the products could be reliably purified by a simple acid–base extraction and subjected to downstream functionalization (see Scheme 5).[17]

The divergent regioselectivity observed for substituted arenes was unexpected based on our previous studies involving Pd- and Ni-catalyzed dearomative functionalization,[11] and warranted further investigation into the origins of selectivity. We performed density functional theory (DFT) calculations to investigate the reaction energy profiles of the CuH-catalyzed dearomative hydroamination of trifluorotoluene (**1f**) and *tert*-butylbenzene (**1b**) (Figures 1a and S2). The trifluoromethyl-substituted MTAD–benzene cycloadduct (**3f**) undergoes facile hydrocupration with the IMes-supported monomeric LCuH (**7**) via **TS1f-1** ($\Delta G^{\ddagger}$ = 8.1 kcal/mol with respect to the dimeric CuH resting state **6**[19]) to form alkyl copper species **8f-1**. Intermediate **8f-1** undergoes β-elimination (**TS2f**) to form π–alkene copper complex **9f**, which then isomerizes to a more stable complex **10f**. Because hydrocupration is exothermic and irreversible, this step determines the product regioselectivity. In the reaction with the CF_3-substituted **3f**, the most favorable hydrocupration pathway is the 2,1-insertion with the more electron-deficient alkene[20] that forms a Cu–C bond with the CF_3-substituted alkenyl carbon (**TS1f-1**, Figure 1b). Here, the electron-withdrawing CF_3 substituent stabilizes the partial negative charge building up at the α-carbon in both **TS1f-1** and the resulting tertiary alkyl copper species **8f-1**. No unfavorable steric repulsions between the CF_3 substituent and the monodentate IMes ligand were observed in **TS1f-1**. Instead, favorable C–F···H–C non-covalent interactions[21] between the CF_3 group on the alkene and the *ortho*-Me substituents on IMes (2.57 and 2.60 Å) further stabilize **TS1f-1**. Such stabilizing non-cova-

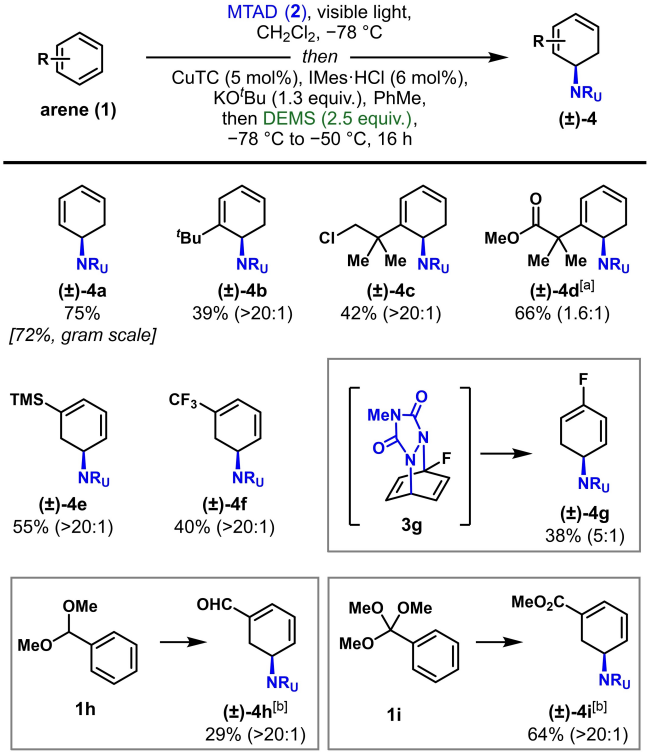

Scheme 2. Mononuclear arene scope for Cu-catalyzed dearomative 1,2-hydroamination. Standard reaction conditions: MTAD (**2**, 0.5 mmol, 1.0 equiv), arene (5.0 mmol, 10 equiv.), CH_2Cl_2 (0.1 M), visible light, −78 °C, 12 h; then solution of catalyst [CuTC (5 mol %), IMes·HCl (6 mol %), KO^{t}Bu (1.3 equiv.), PhMe (2.0 mL)]; then DEMS (2.5 equiv.) added slowly dropwise. Reported yields were determined by ^{1}H NMR of reaction mixtures after acid–base extraction using 0.167 mmol of nitromethane as internal standard with ratio of constitutional isomers in parentheses. [a] Reaction temperature of −78 °C to −20 °C. [b] Based on crude NMR analysis, the acetal and orthoester protecting groups were hydrolyzed during workup to provide the products **4h** and **4i**.

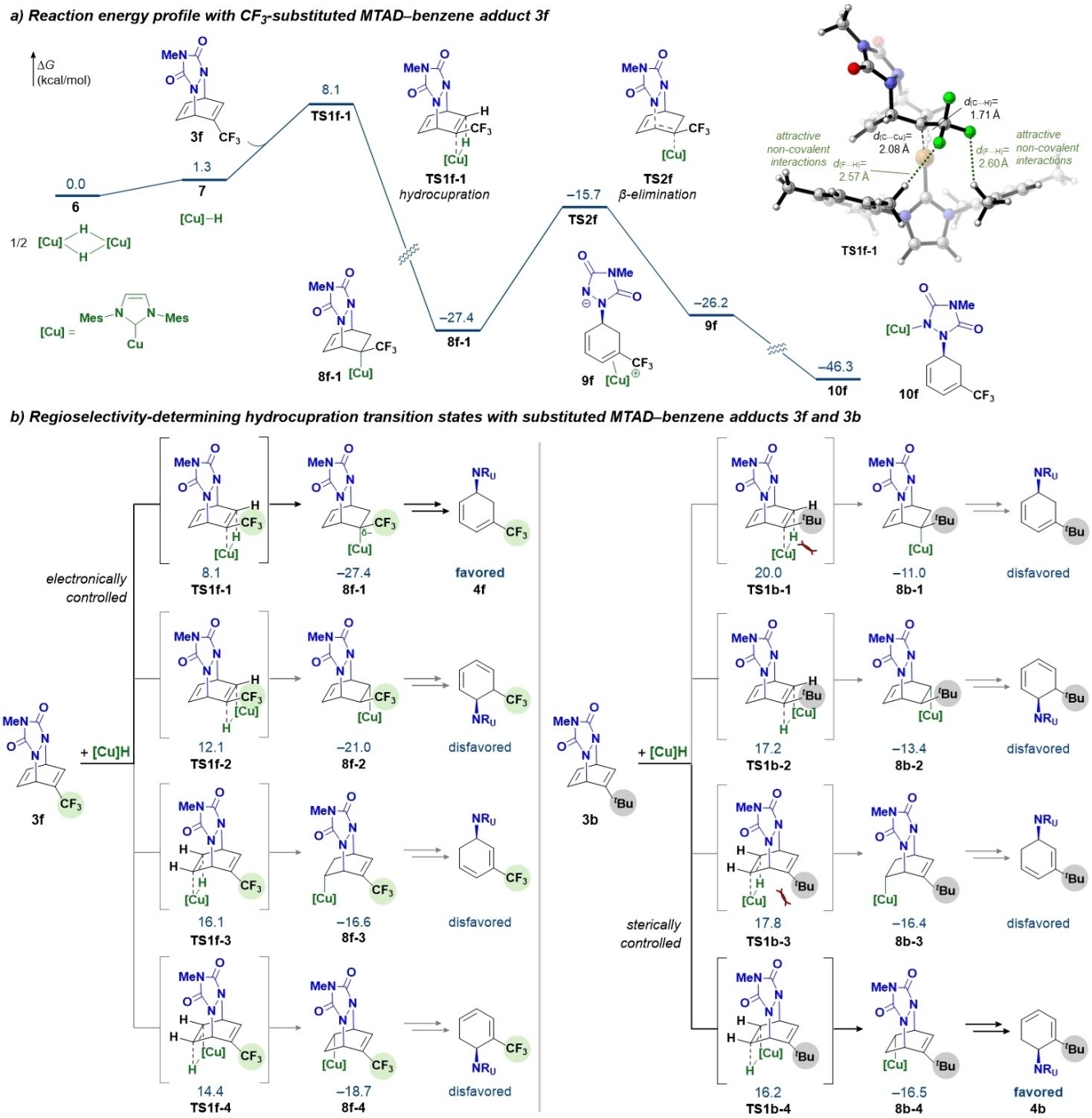

Figure 1. (a) Computational study of the reaction mechanism. (b) Computational study for observed regioselectivities. All Gibbs free energies are in kcal/mol with respect to the dimeric $[LCuH]_2$ resting state (**6**, L = IMes) and the MTAD–benzene adduct. DFT calculations were performed at the M06/SDD-6-311 + G(d,p)/SMD(CH_2Cl_2)//B3LYP/SDD-6-31G(d) level of theory.

lent interactions are absent in regioisomers **TS1f-2**, **TS1f-3**, and **TS1f-4**, where the CF_3 substituents are placed further away from the IMes ligand (Figure S5). Our DFT calculations indicate that the hydrocupration with the TMS-substituted MTAD–benzene adduct **3e** occurs with the same regioselectivity preference where the Cu–C bond formation occurs at the TMS-substituted carbon (Figure S4).[22]

Next, we investigated the regioselectivity of the reaction with the *tert*-butyl substituted MTAD–benzene adduct **3b**. Here, the sterically hindered and more electron-rich ^{t}Bu-substituted alkene is less reactive in hydrocupration (**TS1b-1** and **TS1b-2**). The relative stabilities of hydrocupration transition states with the less substituted alkene (**TS1b-3** versus **TS1b-4**) are affected by steric repulsions between the *tert*-butyl substituent and the Cu catalyst. **TS1b-4**, where the Cu is placed furthest away from the *tert*-butyl group, is the most favorable and eventually leads to the experimentally observed constitutional isomer **4b**. The steric repulsions in

the less favorable **TS1b-3** are evidenced by the distortion of the IMes ligand, which deviates from the planar geometry at the Cu center (Figure S3). Taken together, the DFT calculations indicate that electronic and steric effects during hydrocupration lead to the divergent regioselectivity of the dearomative hydroamination of substituted arenes–alkyl-substituted arenes favor Cu–C bond formation at the *para* position to minimize steric repulsion, whereas CF_3– and TMS-substituted arenes favor Cu–C bond formation at the electronically activated *ipso* position.

In addition to exploring the capabilities of the dearomative 1,2-hydroamination with benzene derivatives, we tested various polynuclear aromatics (Scheme 3). Using nearly identical conditions as those optimized for benzene, naphthalene-derived **12a** was synthesized in 52 % yield, and 49 % yield on gram scale. Aryl ester and halide substituents were tolerated under the reaction conditions, with **12b** and **12c** isolated in moderate yield. Trimethylsilyl-, nitro-, and aryl substituents were also compatible with the present dearomative 1,2-hydroamination, providing **12d**–**12g** in serviceable yields, albeit with a range of regioselectivity values. Heterocycles reacted productively to form **12h**–**12j**, with the carbocyclic ring exclusively undergoing dearomative functionalization in accordance with our previous findings.[10,11]

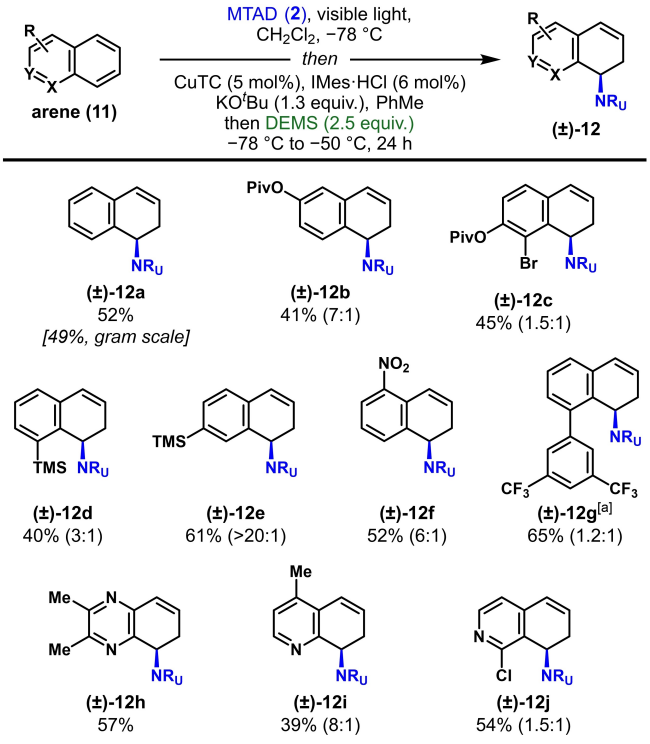

Scheme 3. Polynuclear arene scope for Cu-catalyzed dearomative 1,2-hydroamination. Standard reaction conditions: MTAD (**2**, 0.5 mmol, 1.0 equiv), arene (1.0 mmol, 2.0 equiv.), CH_2Cl_2 (0.1 M), visible light, −78 °C, 12 h; then solution of catalyst [CuTC (5 mol%), IMes·HCl (6 mol%), KO^{t}Bu (1.3 equiv.), PhMe (2.0 mL)]; then DEMS (2.5 equiv.) added slowly dropwise. Reported yields are of isolated products, with ratio of constitutional isomers (in parentheses) determined by ^{1}H NMR of the crude reaction mixtures. [a] Reaction temperature of −78 °C to −20 °C. Piv = pivaloyl.

Enantioselective Dearomative 1,2-Hydroamination

Having synthesized a variety of racemic dearomatized products using this methodology, we next turned our attention to exploring desymmetrization of the arene–arenophile cycloadduct intermediates (Scheme 4). During our recent studies toward the total synthesis of ribostamycin (**5**, Figure 1b), ferrocene-derived bisphosphine ligand TaniaPhos (**13**) was found to provide the highest level of enantioinduction, with product **4a** obtained in 69 % yield and 96:4 er.[12] Unfortunately, due to the relatively lengthy synthetic sequence towards **13** and its high commercial price,[23] this ligand could be cost-prohibitive to employ in the large-scale dearomative 1,2-hydroamination. As such, another aim of this work was to identify a more economical variant to provide comparable enantioinduction on benzene. Additional screening focused on an NHC-based framework identified ligand **14** as optimal (see Supporting Information, Table S3, for full optimization details).[24] This NHC ligand provided **4a** with the same level of enantioinduction (96:4 er) as TaniaPhos (**13**) with slightly improved yield and the additional benefits of a lower cost and facile synthesis.[25] Importantly, this reaction could be successfully conducted on multigram scale without any erosion in yield or selectivity (see Supporting Information for details). However, in further studies this ligand proved to be inefficient for desymmetrization of naphthalene (**11a**) and 2,3-dimeth-

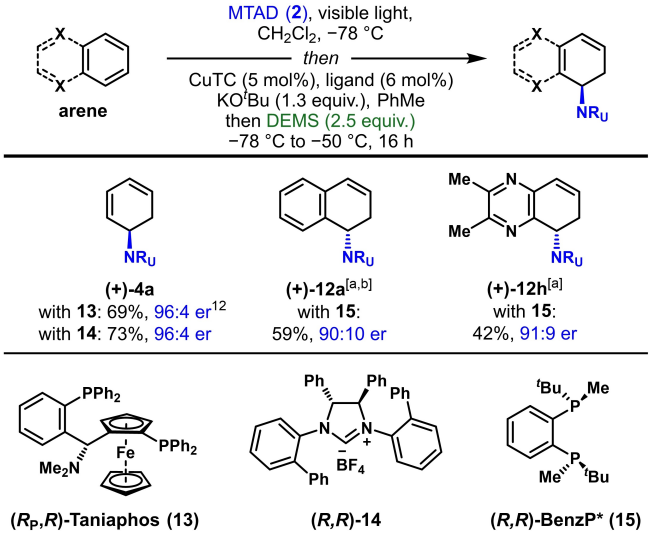

Scheme 4. Cu-catalyzed enantioselective dearomative 1,2-hydroamination. Standard reaction conditions: MTAD (**2**, 0.5 mmol, 1.0 equiv), arene [5.0 mmol (10 equiv.) for **4a** or 1.0 mmol (2.0 equiv.) for **12a** and **12h**], CH_2Cl_2 (0.1 M), visible light, −78 °C, 12 h; then solution of catalyst [CuTC (5 mol%), ligand (6 mol%), KO^{t}Bu (1.3 equiv.), PhMe (2.0 mL)]; then DEMS (2.5 equiv.) added slowly dropwise. Reported yields were determined by ^{1}H NMR of reaction mixtures after acid–base extraction using nitromethane as internal standard. [a] Reaction time of 24 h. [b] Reaction temperature of −78 °C to −20 °C.

ylquinoxaline (**11h**). Therefore, additional investigation of chiral ligands identified the ligand BenzP* (**15**) as suitable,[26] providing enantioenriched products **12a** and **12h** in 90:10 and 91:9 er, respectively.

Derivatization Studies

With dearomatized hydroamination products **4a** and **12a** both accessible on a gram scale, we focused our efforts on the selective functionalization of the diene and styrene moieties to provide stereochemically diverse, polysubstituted cyclohexylamines and derivatives (Scheme 5). Thus, benzene-derived diene **4a** was converted to cyclic carbamate **16**, using a photochemical [4+2]-cycloaddition with $^1O_2$ as a key functionalization step.[27] Similarly, hetero-Diels–Alder between **4a** and nitrosobenzene furnished *trans*-1,2-amino alcohol **17** after hydrogenolysis and urazole hydrolysis.[28] Additionally, a chemo- and diastereoselective dihydroxylation of diene **4a** afforded acetonide **18**, which could be elaborated to aminodiol **19**. Importantly, the urazole motif could also undergo oxidation using *tert*-butyl hypochlorite, providing enone **20**.

On the other side, dihydroxylation of 1,2-hydroaminated naphthalene **12a**, acetonide protection, and urazole hydrolysis provided aminodiol **21**. Additionally, a sequence involving Rh-catalyzed hydroboration and oxidation led to the *trans*-1,4-amino alcohol **22** with excellent diastereoselectivity (>20:1 dr).[29] A sequence involving *anti*-epoxidation followed by intramolecular epoxide opening produced a mixture of separable constitutional isomers **23** and **24**, in approximately 3:1 ratio. Each of these bicyclic urazole intermediates were brought forward respectively to *syn*-1,3-diamine **25** and *syn*-1,4-diamine **26** after hydrazinolysis and hydrogenation.[10a] These densely functionalized aliphatic amines were rapidly produced from aromatic hydrocarbon feedstocks, highlighting the utility of dearomative 1,2-hydroamination.

Conclusions

In conclusion, we have developed a Cu-catalyzed 1,2-hydroamination of nonactivated arenes using an arenophile-based dearomatization platform. This strategy features an arenophile-based cycloaddition followed by catalytic hydrocupration with concurrent opening of the urazole cycloadduct. This method delivers products with exclusive 1,2-selectivity. Several feedstock arenes, such as benzene, trifluorotoluene, and a benzaldehyde derivative, as well as naphthalene, quinoline, and isoquinoline derivatives were suitable substrates for this transformation. In several cases with substituted benzenes, we observed a unique divergence of regioselectivity which was rationalized using DFT calculations. These studies pointed to a delicate balance between electronic and steric effects during the hydrocupration event. Furthermore, we developed a new practical protocol for enantioselective hydroamination of benzene, which was validated on a gram scale. Similarly, this asymmetric approach could also be extended to naphthalene and quinoxaline substrates. Finally, given that this dearomative strategy provides direct access to products that are not readily available by any other chemical or chemoenzymatic means, we demonstrated its synthetic potential through further elaborations. These efforts resulted in rapid access to a broad range of small, polyfunctionalized building blocks

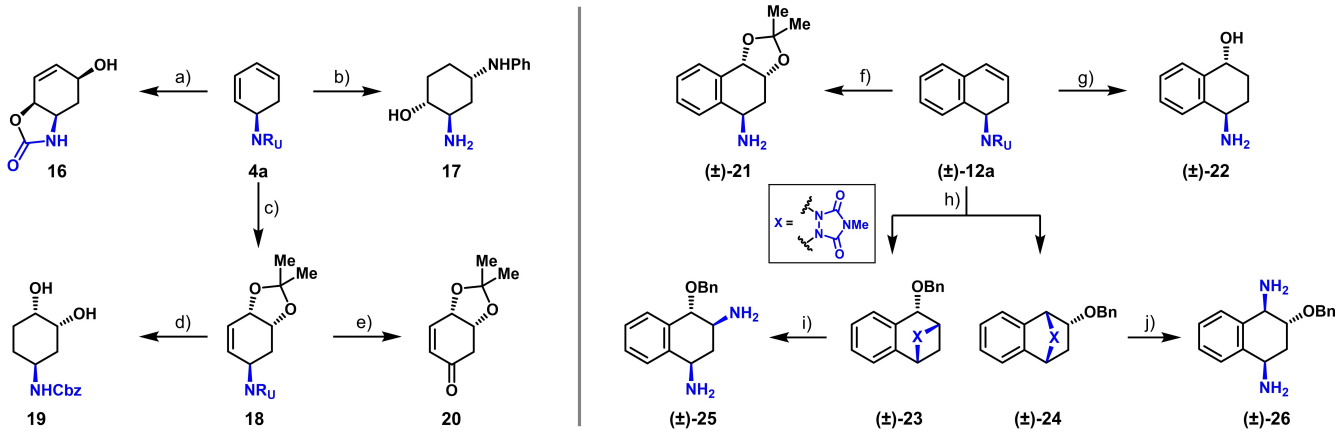

Scheme 5. Derivatization of benzene- and naphthalene-derived products **4a** and **12a**. Reagents and conditions: (a) (i.) α-bromoacetophenone, K_2CO_3, 57%; (ii.) tetraphenylporphyrin (cat.), O_2, visible light, 58%, 3:1 dr; (iii.) thiourea, 77%; (iv.) KOH, 38%; (b) (i.) α-bromoacetophenone, K_2CO_3, 57%; (ii.) PhNO, 87%, 10:1 dr; (iii.) Pt(S)/C (cat), H_2, then KOH, 49%; (c) OsO_4 (cat.), NMO, then 2,2-DMP, TsOH, 81%, >20:1 dr; (d) (i.) Crabtree's catalyst, H_2, 96%; (ii.) α-bromoacetophenone, K_2CO_3, 77%; (iii.) KOH, then CbzCl, 71% (e) ^{t}BuOCl, 70%; (f) (i.) α-bromoacetophenone, K_2CO_3, 61%; (ii.) OsO_4 (cat.), NMO, citric acid, 78%, >20:1 dr; (iii.) 2,2-DMP, TsOH, 85%; (iv.) KOH, 54% (g) (i.) α-bromoacetophenone, K_2CO_3, 61%; (ii.) $Rh(cod)_2BF_4$ (cat.), BINAP (cat.), HBcat, then $NaBO_3$, 58%, >20:1 dr; (iii.) KOH, 50%; (h) (i.) Boc_2O, DMAP (cat.), then *m*CPBA, 57%, >20:1 dr; (ii.) Na_2CO_3, then NaH, BnBr, 54% of **23** and 20% of **24**; (i) NH_2NH_2, then Raney-Ni (cat.), H_2, 79%; (j) NH_2NH_2, then Raney-Ni (cat.), H_2, 66%. NMO = *N*-methylmorpholine-*N*-oxide; 2,2-DMP = 2,2-dimethoxypropane; TsOH = *p*-toluenesulfonic acid; Cbz = benzyloxycarbonyl; cod = 1,5-cyclooctadiene; cat = catechol; Boc = *tert*-butoxycarbonyl; DMAP = 4-dimethylaminopyridine; *m*CPBA = *meta*-chloroperoxybenzoic acid.

bearing heteroatom functionality. Further studies regarding the expansion of this reactivity and applications to synthesis of natural products are ongoing in our laboratory.

Supporting Information

Detailed experimental procedures, spectroscopic data, computational data, and ^{1}H, ^{13}C, and ^{19}F NMR spectra are available in the Supporting Information of this article. Cartesian coordinates of optimized geometries are also provided. The authors have cited additional references within the Supporting Information.

Acknowledgements

Financial support for this work was provided by the NIH/National Institute of General Medical Sciences (GM122891 to D.S. and R35GM128779 to P.L.). DFT calculations were carried out at the University of Pittsburgh Center for Research Computing and the Advanced Cyberinfrastructure Coordination Ecosystem: Services & Support (ACCESS) program, supported by NSF award numbers OAC-2117681, OAC-1928147 and OAC-1928224. We also thank Dr. D. Olson and Dr. L. Zhu for NMR spectroscopic assistance, Dr. D. L. Gray for X-ray crystallographic analysis assistance, and F. Sun for mass spectrometric assistance.

Conflict of Interest

The authors declare no conflict of interest.

Data Availability Statement

The data that support the findings of this study are available in the supplementary material of this article.

Keywords: arenes · arenophiles · dearomatization · copper · hydroamination

[1] a) S. D. Roughley, A. M. Jordan, *J. Med. Chem.* **2011**, *54*, 3451; b) E. Vitaku, D. T. Smith, J. T. Njardarson, *J. Med. Chem.* **2014**, *57*, 10257.

[2] A. Trowbridge, S. M. Walton, M. J. Gaunt, *Chem. Rev.* **2020**, *120*, 2613.

[3] For a detailed review of transition-metal catalyzed hydroamination, see: L. Huang, M. Arndt, K. Gooßen, H. Heydt, L. J. Gooßen, *Chem. Rev.* **2015**, *115*, 2596.

[4] For selected examples, see: a) M. Utsunomiya, J. F. Hartwig, *J. Am. Chem. Soc.* **2003**, *125*, 14286; b) Y. Miki, K. Hirano, T. Satoh, M. Miura, *Angew. Chem. Int. Ed.* **2013**, *52*, 10830; c) S. Zhu, N. Niljianskul, S. L. Buchwald, *J. Am. Chem. Soc.* **2013**, *135*, 15746; d) Y. Yang, S.-L. Shi, D. Niu, P. Liu, S. L. Buchwald, *Science* **2015**, *349*, 62; e) J. Gui, C.-M. Pan, Y. Jin, T. Qin, J. C. Lo, B. J. Lee, S. H. Spergel, M. E. Mertzman, W. J. Pitts, T. E. La Cruz, M. A. Schmidt, N. Darvatkar, S. R. Natarajan, P. S. Baran, *Science* **2015**, *348*, 886; f) A. J. Mussachio, B. C. Lainhart, X. Zhang, S. G. Naguib, T. C. Sherwood, R. R. Knowles, *Science* **2017**, *355*, 727; g) D. C. Miller, J. M. Ganley, A. J. Mussachio, T. C. Sherwood, W. R. Ewing, R. R. Knowles, *J. Am. Chem. Soc.* **2019**, *141*, 16590.

[5] For state-of-the-art approaches and challenges in this area, see: a) W. C. Wertjes, E. H. Southgate, D. Sarlah, *Chem. Soc. Rev.* **2018**, *47*, 7996; b) C. J. Huck, D. Sarlah, *Chem* **2020**, *6*, 1589.

[6] For recent examples, see: a) X. Ma, J. J. Farndon, T. A. Young, N. Fey, J. F. Bower, *Angew. Chem. Int. Ed.* **2017**, *56*, 14531; b) E. Lee, Y. Hwang, Y. B. Kim, D. Kim, S. Chang, *J. Am. Chem. Soc.* **2021**, *143*, 6363; c) S.-G. Wang, Q. Yin, C.-X. Zhuo, S.-L. You, *Angew. Chem. Int. Ed.* **2015**, *54*, 647; d) C. Jing, J. J. Farndon, J. F. Bower, *Chem. Rec.* **2021**, *21*, 2909.

[7] a) D. Bryce-Smith, A. Gilbert, C. Manning, *Angew. Chem. Int. Ed.* **1974**, *13*, 341; b) M. Bellas, D. Bryce-Smith, M. T. Clarke, A. Gilbert, G. Klunkin, S. Krestonosich, C. Manning, S. Wilson, *J. Chem. Soc. Perkin Trans. 1* **1977**, *23*, 2571.

[8] a) L. A. P. Kane-Maguire, E. D. Honig, D. A. Sweigart, *Chem. Rev.* **1984**, *84*, 525; b) K. B. Wilson, H. S. Nedzbala, S. R. Simpson, M. N. Ericson, K. S. Westendorff, M. D. Chordia, D. A. Dickie, W. D. Harman, *Helv. Chim. Acta* **2021**, *104*, e2100103; c) Z.-J. Li, M.-Y. Wang, C.-Q. Li, W.-L. Zeng, W. Li, *Chem. Eur. J.* **2023**, *29*, e202300776. For dearomative hydrofunctionalization reactions also employing silane nucleophiles, see: d) J.-Y. Qiu, W.-L. Zeng, H. Xie, M.-Y. Wang, W. Li, *Angew. Chem. Int. Ed.* **2023**, *62*, e202218961; e) C.-Q. Li, X. Jiang, M.-Y. Wang, W.-L. Zeng, W. Li, *CCS Chem.* **2024**, accepted, DOI: 10.31635/ccschem.023.202303573.

[9] a) E. H. Southgate, J. Pospech, J. Fu, D. R. Holycross, D. Sarlah, *Nat. Chem.* **2016**, *8*, 922; b) K. Ikeda, R. Kojima, K. Kawai, T. Murakami, T. Kikuchi, M. Kojima, T. Yoshino, S. Matsunaga, *J. Am. Chem. Soc.* **2023**, *145*, 9326; c) S. Pradhan, F. Mohammadi, J. Bouffard, *J. Am. Chem. Soc.* **2023**, *145*, 12214.

[10] a) M. Okumura, S. Nakamata Huynh, J. Pospech, D. Sarlah, *Angew. Chem. Int. Ed.* **2016**, *55*, 15910; b) D. G. Dennis, M. Okumura, D. Sarlah, *J. Am. Chem. Soc.* **2019**, *141*, 10193; c) Z. Siddiqi, W. C. Wertjes, D. Sarlah, *J. Am. Chem. Soc.* **2020**, *142*, 10125; d) P. Piacentini, T. W. Bingham, D. Sarlah, *Angew. Chem. Int. Ed.* **2022**, *61*, e202208014.

[11] a) M. Okumura, A. S. Shved, D. Sarlah, *J. Am. Chem. Soc.* **2017**, *139*, 17787; b) L. W. Hernandez, U. Klöckner, J. Pospech, L. Hauss, D. Sarlah, *J. Am. Chem. Soc.* **2018**, *140*, 4503; c) W. C. Wertjes, M. Okumura, D. Sarlah, *J. Am. Chem. Soc.* **2019**, *141*, 163; d) C. Tang, M. Okumura, Y. Zhu, A. Hooper, Y. Lee, D. Sarlah, *Angew. Chem. Int. Ed.* **2019**, *58*, 10245; e) C. Tang, M. Okumura, H. Deng, D. Sarlah, *Angew. Chem. Int. Ed.* **2019**, *58*, 15762; f) C. W. Davis, T. W. Bingham, M. Okumura, D. Sarlah, *Synthesis* **2021**, *53*, 4290.

[12] C. N. Ungarean, P. Galer, Y. Zhang, K. S. Lee, J. M. Ngai, S. Lee, P. Liu, D. Sarlah, *Nature Synth.* **2022**, *1*, 542.

[13] a) C. Deutsch, N. Krause, B. H. Lipshutz, *Chem. Rev.* **2008**, *108*, 2916; b) V. Jurkauskas, J. P. Sadighi, S. L. Buchwald, *Org. Lett.* **2003**, *5*, 2417.

[14] a) R. Y. Liu, S. L. Buchwald, *Acc. Chem. Res.* **2020**, *53*, 1229; b) F. Lazreg, C. S. J. Cazin in *N-Heterocyclic Carbenes – Effective Tools for Organometallic Synthesis* (Ed.: S. P. Nolan), Wiley-VCH, Mannheim, **2014**, pp. 199–242.

[15] a) The *tert*-butoxide anion is a privileged ligand in copper hydride catalysis due to the favorable solubility, stability, and transmetallation reactivity of copper *tert*-butoxide complexes, see: T. Tsuda, T. Hashimoto, T. Saegusa, *J. Am. Chem. Soc.* **1972**, *94*, 658; b) < Significant counterion effects have been previously documented in copper hydride catalysis, see: B. H. Lipshutz, C. H. Caires, P. Kuipers, W. Chrisman, *Org. Lett.* **2003**, *5*, 3085.

[16] A complex relationship between silane substituents and transmetallation reactivity is precedented in copper hydride catalysis, see: B. H. Lipshutz, K. Noson, W. Chrisman, A. Lower, *J. Am. Chem. Soc.* **2003**, *125*, 8779.
[17] For a more detailed discussion on product stability and operational details, see the Supporting Information.
[18] Low-temperature NMR studies support the symmetric cycloadduct **3g** depicted in Scheme 2, as only 4 distinct proton signals were associated with the major constitutional isomer present in solution. The origins of this unusual regioselectivity are not clear, but we speculate that the orbital density on the singly-occupied molecular orbital (SOMO) of fluorobenzene during cycloaddition favors the bridgehead-substituted **3g**, and that this selectivity may be further enabled by the small steric size of fluorine.
[19] Y. Xi, J. F. Hartwig, *J. Am. Chem. Soc.* **2017**, *139*, 12758.
[20] L. Hu, H. Gao, Y. Hu, Y.-B. Wu, X. Lv, G. Lu, *J. Org. Chem.* **2023**, *88*, 2750.
[21] a) K. Reichenbächer, H. I. Süss, J. Hulliger, *Chem. Soc. Rev.* **2005**, *34*, 22; b) A. A. Thomas, K. Speck, I. Kevlishvili, Z. Lu, P. Liu, S. L. Buchwald, *J. Am. Chem. Soc.* **2018**, *140*, 13976.
[22] For a detailed discussion on the origin of regioselectivity in the hydrocupration of alkenyl silanes, see: N. Niljianskul, S. Zhu, S. L. Buchwald, *Angew. Chem. Int. Ed.* **2015**, *54*, 1638.
[23] a) K. Tappe, P. Knochel, *Tetrahedron: Asymmetry* **2004**, *15*, 91; b) At the time of writing, the cost of Taniaphos is over $700 USD/gram through MilliporeSigma.
[24] a) V. Lillo, A. Prieto, A. Bonet, M. M. Díaz-Requejo, J. Ramírez, P. J. Pérez, E. Fernández, *Organometallics* **2009**, *28*, 659; b) K.-S. Lee, A. H. Hoveyda, *J. Org. Chem.* **2009**, *74*, 4455.
[25] Several improvements were made to the reported synthetic route towards ligand **(*R*,*R*)-14** to further increase scalability, see Supporting Information for details.
[26] T. Imamoto, K. Tamura, Z. Zhang, Y. Horiuchi, M. Sugiya, K. Yoshida, A. Yanagisawa, I. D. Gridney, *J. Am. Chem. Soc.* **2012**, *134*, 1754.
[27] The unexpected *syn*-selective hetero-Diels–Alder reaction with $^1O_2$ can be rationalized by invoking the Cieplak effect, since the anti-periplanar C–H bond is a better hyperconjugative donor than the C–N bond: a) J. M. Coxon, D. Q. McDonald, *Tetrahedron Lett.* **1992**, *33*, 651; b) S. Kim, M. A. Ciufolini, *Org. Lett.* **2011**, *13*, 3274.
[28] W. Adam, A. Pastor, T. Wirth, *Org. Lett.* **2000**, *2*, 1295.
[29] T. Hayashi, Y. Matsumoto, Y. Ito, *J. Am. Chem. Soc.* **1989**, *111*, 3426.

Manuscript received: April 16, 2024
Accepted manuscript online: May 23, 2024
Version of record online: July 16, 2024